Nanoscale Res Lett (2009) 4:1267–1270
DOI 10.1007/s11671-009-9391-x

NANO EXPRESS

Nanocapsule for Safe and Effective Methane Storage

M. V. Suyetin · A. V. Vakhrushev

Received: 1 June 2009 / Accepted: 3 July 2009 / Published online: 17 July 2009

Abstract A nanocapsule for safe and effective methane storage is investigated by the method of molecular dynamics. The mass content of methane in the nanocapsule reaches the value of 14.5 mass%. The nanocapsule consists of two parts: a locking chamber and a storage area. The locking chamber is the nanotube (10.10), open at one end, with a $K@C_{60}^{1+}$ endohedral complex inside it. The storage area is a nanotube (20.20). The locking chamber and the storage area are joined with each other and form T-junction. The locking chamber is opened at the methane filling and the discharge stages, and it is closed at the storage stage. Thanks to the locking chamber, methane molecules are stored in the nanocapsules under normal external conditions. Opening and closing of the locking chamber are carried out by the $K@C_{60}^{1+}$ endohedral complex displacement, which is done by the electric field action. The specific structure of the nanocapsule allows two aims to be reached: a high methane mass content and significant level of safety.

Keywords Molecular dynamics · Nanocapsules · Methane storage

Introduction

Synthesizing a bucky shuttle or a nanopeapod [1, 2], consisting of a nanotube [3] and fullerene [4] has opened new horizons of investigations into the properties of nanostructures for researchers. At present time it is supposed, that bucky shuttles can be used, for example, as nanosized memory elements [5] or to serve as a basis for creating devices for target drug delivery [6]. One of the most promising directions of nanocapsule usage is its exploitation as a nanoscale container or a capsule for different gases storage [7–11], because conventional nanotubes cannot meet the requirements of industrial use, in spite of having numerous special improvements in their structure [12–14]. Using nanostructured carbon engineering [15–17], opens new prospects for creating nanocapsules of complex structural forms.

In the present work, the nanocapsule for methane storage by the method of molecular dynamics is investigated. The nanocapsule consists of two nanotubes of different diameters joined with each other, forming T-junction. The bigger nanotube—(20.20) presents the area of methane storage. The smaller one—(10.10) has a hole for a methane molecule penetration and the $K@C60^{1+}$ endohedral complex and also plays the role of "a locking chamber". The position of the $K@C60^{1+}$ ion in the locking chamber is ruled by the electric field action and defines the state of the chamber—opened or closed access for methane molecules into the nanocapsule.

The performed calculations show that the usage of nanocapsules of complex structural forms is a new way of effective and safe storage of methane.

Computational Model and Details

The objects of the investigation are a nanocapsule, the $K@C_{60}^{1+}$ endohedral complex and methane molecules. The nanocapsule consists of the locking chamber and storage area. The area of the methane molecules storage is a nanotube (20.20). The locking chamber is a nanotube

M. V. Suyetin (✉) · A. V. Vakhrushev
Institute of Applied Mechanics Ub RAS, T. Baramzinoy Str., 34, 426006 Izhevsk, Russia
e-mail: msuyetin@gmail.com

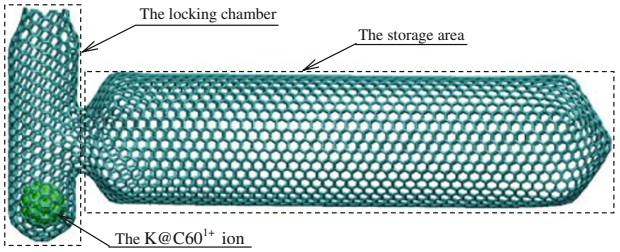

Fig. 1 The nanocapsule for methane molecules storage consists of the locking chamber and storage area

(10.10) containing a $K@C_{60}^{1+}$ ion. One end of the locking chamber is opened and the $K@C_{60}^{1+}$ ion cannot leave the nanocapsule under the action of the electric field, because the diameter of the nanotube (10.10) end is smaller than the $K@C_{60}^{1+}$ ion diameter, but the hole is large enough for methane molecule penetration. In Fig. 1, the nanocapsule is shown, one can also see the locking chamber, the storage area of the nanocapsule and the $K@C_{60}^{1+}$ ion.

Molecular dynamics simulation of filling, storage, discharge processes and the $K@C_{60}^{1+}$ ion displacement under the action of the electric field were performed by NAMD program [18]. The visualization of the calculated results was performed with VMD program [19]. The value of the time step for simulation is 1 fs. The values of the atomic charges in the methane molecule are as follows: a carbon atom is −0.628203 Mulliken and a hydrogen atom is +0.157051 Mulliken [11]. The charge of $+1e$ of the $K@C_{60}^{1+}$ endohedral complex is uniformly distributed over the C_{60} shell.

The position of the $K@C_{60}^{1+}$ ion in the locking chamber is defined by the action of the electric field. The electric field vector is parallel to the locking chamber walls. The value of the electric field intensity needed for the $K@C_{60}^{1+}$ ion displacement is 5.655×10^9 V/M. The $K@C_{60}^{1+}$ ion position defines the ability of the methane molecules to penetrate into the nanocapsule.

Results and Discussion

The molecular dynamics simulation of the nanocapsule filling by methane molecules takes place under T=300 K and external pressure 20 MPa. The locking chamber is opened as shown in Fig. 1, i.e., the $K@C_{60}^{1+}$ ion does not prevent the methane molecules from penetrating into the storage area. Methane molecules freely penetrate into the open end of the locking chamber and then concentrate in the storage area of the nanocapsule. The dynamics of the nanocapsule methane filling is shown in Fig. 2. It is clearly seen that 2.2 ps is enough to complete filling of the storage area of the nanocapsule.

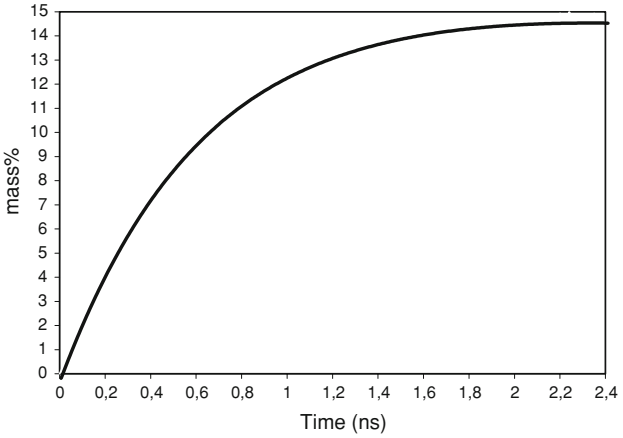

Fig. 2 The results of the molecular dynamics simulation of the nanocapsule methane filling. Thermodynamic conditions are $P = 20$ MPa and $T = 300$ K

In order to start the stage of methane storage, it is necessary to close the locking chamber. To implement this, the $K@C_{60}^{1+}$ ion moves under the action of the electric field and blocks the open end of the locking chamber. The value of the intensity of the electric field needed for moving the $K@C_{60}^{1+}$ ion equals to 5.655×10^9 V/M. This value is extremely large, but we should take into account that the length of the locking chamber is extremely small—46.6 A. In this case, if we suppose that the distance between the plates for the electric field creation is 100 A, the voltage of the electric current, which is essential for this electric field creation, should be only 56 V. The results of our simulation of closing the locking chamber are shown in Fig. 3. The graphs of the $K@C_{60}^{1+}$ ion displacement and change in the $K@C_{60}^{1+}$ ion kinetic energy in the locking chamber under the action of the electric field at the stage of closing are shown. The kinetic energy of the $K@C_{60}^{1+}$ ion is decreased to 2 and 6 ps after the electric field has been applied, because of the necessity to overcome the energetic barriers of the hole situated in the area of junction between the locking chamber and storage area. On the whole, the $K@C_{60}^{1+}$ ion displacement in the locking chamber is almost uniform, and the velocity is in the range of 300–400 m/s. The dramatic decrease of the $K@C_{60}^{1+}$ ion kinetic energy by 9 ps is explained by the $K@C_{60}^{1+}$ ion braking, i.e., the $K@C_{60}^{1+}$ ion kinetic energy is converted into the vibration temperature of the methane molecules, located near the outlet of the locking chamber. Then, we can see how acceleration of the $K@C_{60}^{1+}$ ion and damped oscillations take place when the ion reaches the end of the locking chamber. The $K@C_{60}^{1+}$ kinetic energy is also damping, reaching almost a zero value. Further small oscillations can be simply explained by the thermal vibrations of the atoms of the $K@C_{60}^{1+}$ ion.

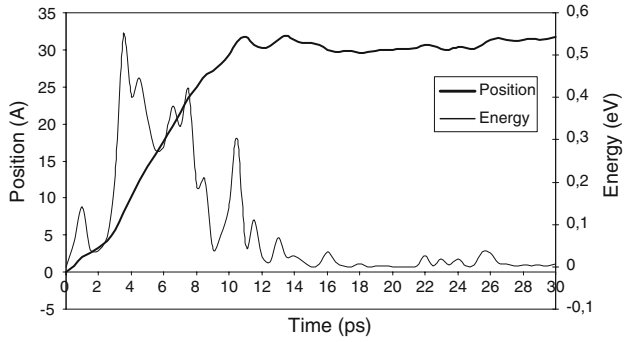

Fig. 3 The results of the molecular dynamics simulation of the $K@C_{60}^{1+}$ ion displacement in the locking chamber under the action of the electric field at the stage of closing. The $K@C_{60}^{1+}$ ion position with respect to the initial (Time = 0 ps) ion position as a function of time. The change in the $K@C_{60}^{1+}$ ion kinetic energy as a function of time

In Fig. 4, the nanocapsule with locked methane molecules in it is shown. The $K@C_{60}^{1+}$ ion is pressed by the methane molecules to the opened end of the nanocapsule after the electric field is switched off. The $K@C_{60}^{1+}$ ion cannot leave the nanocapsule because the diameter of the outlet is smaller than the diameter of the $K@C_{60}^{1+}$ ion. The $K@C_{60}^{1+}$ ion blocks the outlet and the gas molecules cannot leave the nanocapsule. Now the external gas pressure can be greatly reduced down to zero. The temperature is kept the same and equals 300 K. Then, molecular dynamics simulation performed during 500 ns showed that there was no methane leakage and the nanocapsule structure was stable.

In case of need of discharging the methane molecules from the nanocapsule, it is necessary to open the outlet of the locking chamber by the $K@C_{60}^{1+}$ ion under the action of the electric field. The intensity of the electric field is the same as at the stage of closing the locking chamber, but the direction is opposite. The results of our simulation of opening the locking chamber are shown in Fig. 5: the graphs of the $K@C_{60}^{1+}$ ion displacement and change in the $K@C_{60}^{1+}$ ion kinetic energy in the locking chamber under the action of the electric field. The $K@C_{60}^{1+}$ ion under the action of electric field opens the outlet and methane

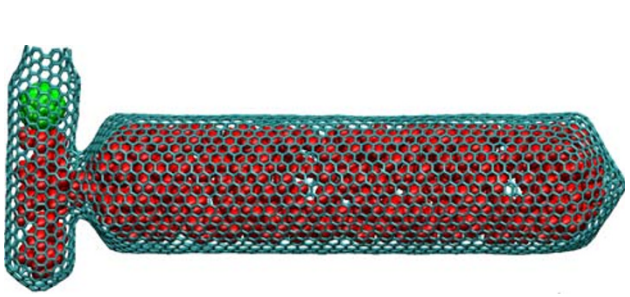

Fig. 4 The nanocapsule is at the stage of the methane molecules storage. The $K@C_{60}^{1+}$ ion is at the upper part of the locking chamber and blocks the outlet

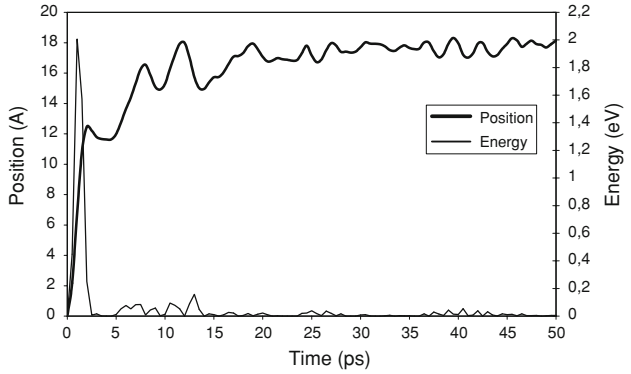

Fig. 5 The results of the molecular dynamics simulation of the $K@C_{60}^{1+}$ ion displacement in the locking chamber under the action of the electric field at the stage of opening. The $K@C_{60}^{1+}$ ion position with respect to the initial (Time = 0 ps) ion position as a function of time. Change in the $K@C_{60}^{1+}$ ion kinetic energy as a function of time

molecules leave the nanocapsule freely. The kinetic energy of the $K@C_{60}^{1+}$ ion grows rapidly during the first few picoseconds, reaching the maximum value of approximately 2 eV. Then the kinetic energy sharply decreases. The kinetic energy is transformed into the vibrational temperature of the methane molecules, situated in the inner part of the locking chamber.

The $K@C_{60}^{1+}$ ion displacement is carried out by jerks, and it blocks a small group of methane molecules in the lower part of the locking chamber, as shown in Fig. 6. The $K@C_{60}^{1+}$ ion is in equilibrium at 25 ps when the electric field influences from one direction and the compressed methane molecules press from the opposite direction. Thus, the outlet of the nanocapsule is opened and methane molecules can leave the nanocapsule freely under the excess pressure inside it.

The methane molecules discharge process is shown in Fig. 7. The thermodynamic conditions of discharge are $T = 300$ K and $P = 0.0$ MPa. One can see that 22 ns is enough for full discharge. The graph of the discharge is very similar to the hyperbola function graph.

If the electric field is switched off during the process of methane molecules escape from the nanocapsule, the

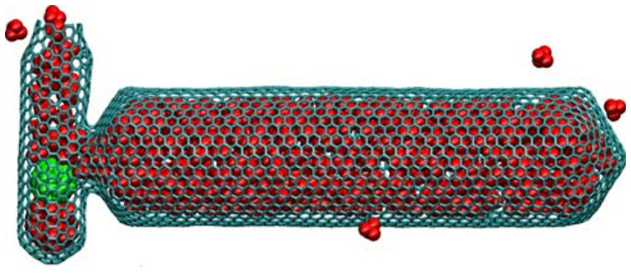

Fig. 6 The nanocapsule is at the stage of methane molecules discharge. The electric field keeps the $K@C_{60}^{1+}$ ion in the lower part of the locking chamber. The methane molecules escape from the nanocapsule freely

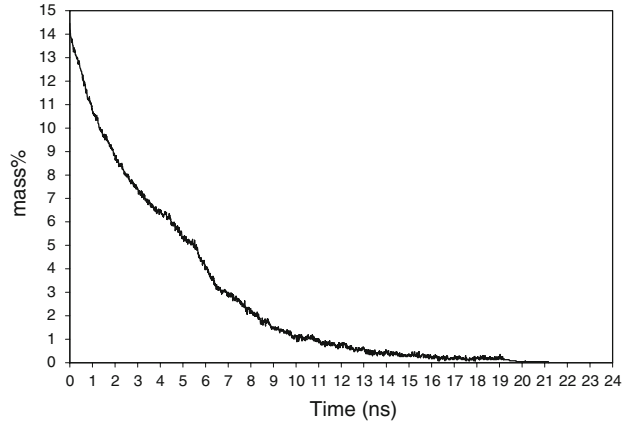

Fig. 7 The results of the molecular dynamics simulation of the methane molecules escape from the nanocapsule. Thermodynamic conditions are $P = 0.0$ MPa and $T = 300$ K

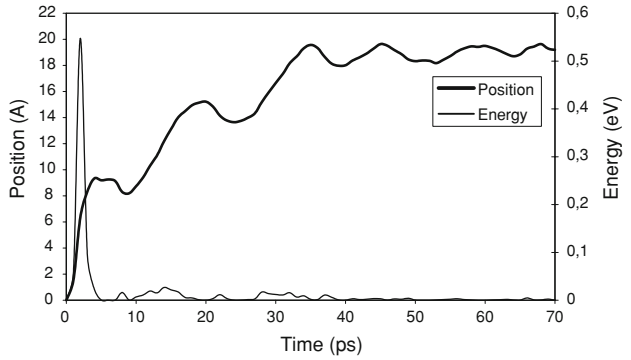

Fig. 8 The results of the molecular dynamics simulation of the $K@C_{60}^{1+}$ ion displacement in the locking chamber under the action of compressed methane molecules. The electric field is switched off. The $K@C_{60}^{1+}$ ion position with respect to the initial (Time = 0 ps) ion position as a function of time. The change in the $K@C_{60}^{1+}$ ion kinetic energy as a function of time

methane molecules compressed by the $K@C_{60}^{1+}$ ion in the lower part of the locking chamber will press the $K@C_{60}^{1+}$ ion, and it will block the outlet of the nanocapsule. In Fig. 8, the graphs of the $K@C_{60}^{1+}$ ion displacement in the locking chamber under the action of the compressed methane molecules and change in the $K@C_{60}^{1+}$ ion kinetic energy are shown. During the first several picoseconds, a significant increase of the $K@C_{60}^{1+}$ kinetic energy takes place, because of the action of the compressed methane molecules. The $K@C_{60}^{1+}$ ion kinetic energy reaches the value of 0,548 eV. However, the $K@C_{60}^{1+}$ ion loses its kinetic energy very fast: it is converted into the vibrational temperature of the methane molecules situated in the upper part of the locking chamber. The $K@C_{60}^{1+}$ ion moves back to the inner part of the locking chamber in approximately 10 ps. It takes place due to the methane molecules from the upper part pushing the $K@C_{60}^{1+}$ ion back. Thus, the $K@C_{60}^{1+}$ ion is pushed from two opposite directions by the methane molecules both in the inner and the upper parts of the locking chamber. This phenomenon forms a wave-like graph of the $K@C_{60}^{1+}$ ion displacement. In the long run, the $K@C_{60}^{1+}$ ion pushes methane molecules from the upper part of the locking chamber and blocks the outlet. The process of the methane molecules escape is interrupted.

Conclusion

We demonstrated the operation of the nanocapsule of a complex structural form suitable for effective methane storage. The nanocapsule under normal conditions retains 14.5 mass% of methane molecules, which were filled up under $T = 300$ K and $P = 20$ MPa. The nanocapsule opening and closing processes are performed by the displacement of the $K@C_{60}^{1+}$ endohedral complex under the action of the electric field. The calculations showed that the nanocapsules of such structure and principles of operation present a new and effective way of methane storage and can be used to store other gases.

References

1. B. Smith, M. Monthioux, D. Luzzi, Nature **396**, 323 (1998)
2. B. Smith, D. Luzzi, Chem. Phys. Lett. **321**, 169 (2000)
3. S. Iijima, Nature **354**, 6348 (1991)
4. H. Kroto, J. Heath, S. O'Brien, R. Curl, R. Smalley, Nature **318**, 6042 (1985)
5. Y. Kwon, D. Tomanek, S. Iijima, Phys. Rev. Lett. **82**, 1470 (1999)
6. D. Baowan, N. Thamwattana, J. Hill, Phys. Rev. B **76**, 155411 (2007)
7. Y. Ren, T. Ng, K. Liew, Carbon **44**, 3 (2006)
8. X. Ye, X. Gu, X. Gong, T. Shing, Z. Liu, Carbon **45**, 2 (2007)
9. R. Barayas-Barrraza, R. Guirado-Lopez, Phys. Rev. B Condens. Matter **66**, 15 (2002)
10. T. Oku, M. Kuno, Diam. Relat. Mater. **12**, 3–7 (2003)
11. A. Vakhrushev, M. Suyetin, Nanotechnology **20**, 125602 (2009)
12. Q. Wang, K. Johnson, J. Chem. Phys. **110**, 11 (1999)
13. V. Simonyan, P. Diep, K. Johnson, J. Phys. Chem. B **11**, 21 (1999)
14. Q. Wang, K. Johnson, J. Phys. Chem. B **103**, 23 (1999)
15. A. Krasheninnikov, F. Banhart, Nat. Mater. **9**, 723 (2007)
16. F. Banhart, J. Li, A. Krasheninnikov, Phy. Rev. B **71**, 24 (2008)
17. F. Banhart, J. Mater. Sci. **41**, 4505 (2006)
18. J. Phillips, R. Braun, W. Wang, J. Gumbart, E. Tajkhorshid, E. Villa, et al., Comput. Chem. **26**, 1781 (2005)
19. W. Humphrey, A. Dalke, K. Schulten, J. Mol. Graph. **14**, 33 (1996)